



## Inclusion of Viscous Dissipation on the Boundary Layer Flow of Cu-TiO<sub>2</sub> Hybrid Nanofluid over Stretching/Shrinking Sheet

Yap Bing Kho<sup>1</sup>, Rahimah Jusoh<sup>1,\*</sup>, Mohd Zuki Salleh<sup>1</sup>, Muhammad Khairul Anuar Mohamed<sup>1</sup>, Zulkhibri Ismail<sup>1</sup>, Rohana Abdul Hamid<sup>2</sup>

<sup>1</sup> Centre for Mathematical Sciences, College of Computing and Applied Sciences, Universiti Malaysia Pahang, Lebuhraya Tun Razak, 26300 Gambang, Kuantan, Pahang, Malaysia

<sup>2</sup> Boundary Layer Research Group, Institute of Engineering Mathematics, Faculty of Applied and Human Sciences, Universiti Malaysia Perlis, Perlis, Malaysia

### ARTICLE INFO

### ABSTRACT

#### Article history:

Received 5 August 2021

Received in revised form 29 September 2021

Accepted 30 September 2021

Available online 27 October 2021

#### Keywords:

Hybrid nanofluid; viscous dissipation;  
dual solution; stability analysis

The effects of viscous dissipation on the boundary layer flow of hybrid nanofluids have been investigated. This study presents the mathematical modelling of steady two dimensional boundary layer flow of Cu-TiO<sub>2</sub> hybrid nanofluid. In this research, the surface of the model is stretched and shrunk at the specific values of stretching/shrinking parameter. The governing partial differential equations of the hybrid nanofluid are reduced to the ordinary differential equations with the employment of the appropriate similarity transformations. Then, Matlab software is used to generate the numerical and graphical results by implementing the *bvp4c* function. Subsequently, dual solutions are acquired through the exact guessing values. It is observed that the second solution adhere to less stableness than first solution after performing the stability analysis test. The existence of viscous dissipation in this model is dramatically brought down the rate of heat transfer. Besides, the effects of the suction and nanoparticles concentration also have been highlighted. An increment in the suction parameter enhances the magnitude of the reduced skin friction coefficient while the augmentation of concentration of copper and titanium oxide nanoparticles show different modes.

## 1. Introduction

The properties of thermal conductivity in heat transfer fluid have been considered as the significant and tremendous research since many years ago. This is due to the rapid growth of technology in various fields such as power plant stations, microelectronic factories, manufacturing and biochemical which required the substantial coolants for effective heat dissipation. After that, it is found that the conventional fluids (water, kerosene, ethylene glycol and many others) are no longer work as an ideal solution for proper coolant due to less efficiency in capability of heat transfer rate and higher time consumption. Therefore, the thermal management is inevitable and this led to

\* Corresponding author.

E-mail address: [rahimahj@ump.edu.my](mailto:rahimahj@ump.edu.my)

<https://doi.org/10.37934/arfmts.88.2.6479>

evolution of the totally new coolants that having advance characteristics of thermal conductivity. In order to go beyond the limitations, the researchers conducted an experiment by dispersing the nano-sized particles into the conventional fluids under a certain physical and chemical processes, which eventually showed the higher thermal conductivity and the term of nanofluids been established [1]. At first, Choi and Eastman [2] are the pioneers in coining the nanofluid and found that the heat transfer rate of nanofluids are totally superior than those of the respective conventional fluids. Afterwards, many relevant of these researches and investigations have been carried out to develop appropriate model that intended for the effective thermal conductivity.

Normally, there are some common nanoparticles that always been used by the researchers which are copper, alumina, silver and metal oxides with the average dimension always within the range of 10-100nm. The size of particles can be considered as one of the crucial parts to determine the effective thermal conductivity of nanofluids since this trend is noticeable at the elevated fluid temperature [3]. Nanofluids are recognised as an ideal solution to replace the base fluids due to the two major factors which are the quantum effects and increment of the relative surface area. These factors improving the thermal conductivity, long-term stability, reduced losing energy, reduction in friction and clogging in fluid flow as well as the homogeneity [4]. Ganvir *et al.*, [5] worked on the heat transfer characteristics in nanofluid and summarised that the nanofluids enhanced the thermal conductivity and affected the heat transfer rate. Chakraborty and Panigrahi [6] concluded that the favourable properties of nanofluids are well beneficial in enhancing the performance compared to the base fluids. Other than the concern of thermal conductivity, Hemmati-Sarapardeh *et al.*, [7] studied the evaluation on viscosity of nanofluids to summarise the accuracy over a wide range of experimental conditions. Bakthavatchalam *et al.*, [8] presented the reviews about the thermophysical properties and cooling efficiency of nanofluids and holding the same view that the heat transfer of nanofluids is more efficient than the base fluids. Latterly, Zhang and Xu [9] discovered the better prediction of thermal conductivity of nanofluids which used the method of computational intelligence to demonstrate a high degree of accuracy and effectiveness.

However, due to the modernization of technologies and the higher demand of supplies, the simple nanofluids may no longer meet the requirement. Hence, researchers came out with an idea of the dispersion of two different nanoparticles through the single or two steps method to replace the existed typical nanofluids, called hybrid nanofluids. Numerous researchers agreed that the hybrid nanofluids could be more remarkable and functional than single nanoparticle fluid if the nanocomposite is sturdy and has good aspect ratio. Based on the studies by Kumar and Arasu [10] and Sajid and Ali [11], the hybrid nanofluids yielded higher enhancement in thermal conductivity than single or mono nanofluid with the appropriate combination of hybrid nanoparticles. Other similar conclusions also agreed that the behaviour of hybrid nanofluids may generate better thermal network as well as the heat transfer coefficient [12-14]. Also, it may possess the rheological properties caused by the synergistic effect [15]. Besides, Shah and Ali [16] highlighted the application of hybrid nanofluids in solar energy and showed the great expedition like extinction coefficient, solar weighted absorption and photothermal conversion efficiency.

On the other hand, the viscous dissipation is also an important factor in the fluid flow. The viscous dissipation depicts the work done by a fluid on vertical plate due to the action of shear forces is transformed into heat. Furthermore, viscous dissipation work as the function of internal friction and dissipating the heat in fluidic materials or liquids. Farooq *et al.*, [17] determined a rising in temperature distribution for regular and hybrid nanofluid after explored the effects of viscous dissipation on entropy generation of hybrid nanofluid flow over nonlinear radially disk. The work of stability analysis of Ag-Cu/water hybrid nanofluid in the presence of viscous dissipation had been done by Jusoh *et al.*, [18]. Jahan *et al.*, [19] combined the impact of viscous dissipation and solar

radiation on mixed convection of hybrid nanofluid and found the higher rate of heat transfer. Besides, augmentation of viscous dissipation also enlarged the skin friction coefficient and Sherwood number [20]. Currently, Venkateswarlu and Narayana [21] numerically explained the significant effects of variable viscosity and viscous dissipation of hybrid nanofluid and found an increase in the temperature distribution profile for the Eckert number that characterise heat transfer dissipation. This finding also supported by Aziz *et al.*, [22] after analysed the effects of viscous dissipation of Powell-Eyring hybrid nanofluid.

As a conclusion, most of the above researchers mentioned and agreed that the critical issue is to maintain the stability of nanofluids in order to reach the optimization on thermal properties. As inspired and continuation work from above mentioned studies, the aim of this study is to investigate the influence of viscous dissipation for Cu-TiO<sub>2</sub> hybrid nanofluid flow. The methodology adopted will reduce the governing partial differential equations into a system of ordinary differential equations and solve the problem through bvp4c. The first and second solution will be carried out as well as the explanation on graphical results. Furthermore, the stability test will be performed to determine which solution is more reliable and satisfying.

## 2. Mathematical Modelling

This study is conducted with adoption of the two dimensional, steady and incompressible viscous flow of a Cu-TiO<sub>2</sub> hybrid nanofluid flow on a stretching/shrinking surface with the fixed origin. The horizontal direction of the stretching/shrinking sheet is denoted as  $x$  – axis whereas the vertical line is represented as  $y$  – axis as illustrated in Figure 1. The wall is considered permeable with  $v = -v_w$ .

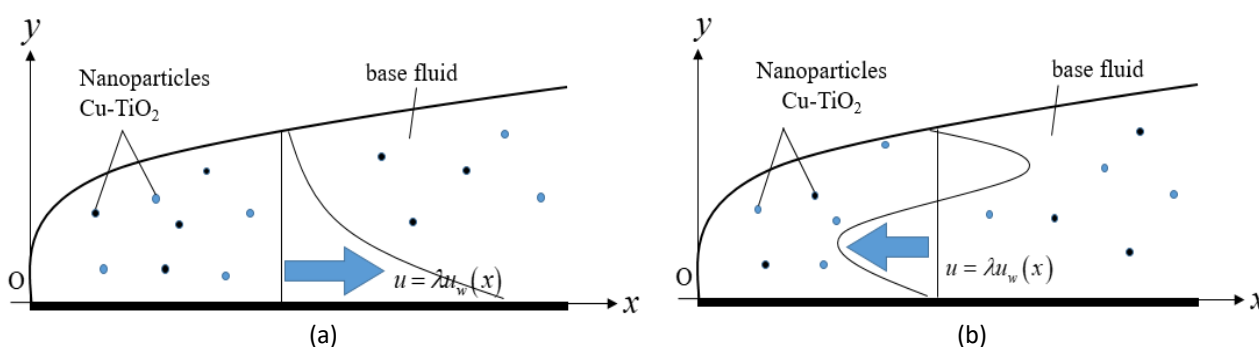


**Fig. 1.** Physical diagram of the hybrid nanofluid model; (a) hybrid nanofluid over stretching sheet ( $\lambda > 0$ ), (b) hybrid nanofluid over shrinking sheet ( $\lambda < 0$ )

By implying the above assumptions, the governing equations of the hybrid nanofluid flow are given as follows:

$$\frac{\partial u}{\partial x} + \frac{\partial v}{\partial y} = 0 \tag{1}$$

$$u \frac{\partial u}{\partial x} + v \frac{\partial u}{\partial y} = \frac{\mu_{hnf}}{\rho_{hnf}} \frac{\partial^2 u}{\partial y^2}, \tag{2}$$

$$u \frac{\partial T}{\partial x} + v \frac{\partial T}{\partial y} = \alpha_{hnf} \frac{\partial^2 T}{\partial y^2} + \frac{\mu_{hnf}}{(\rho C_p)_{hnf}} \left( \frac{\partial u}{\partial y} \right)^2, \tag{3}$$

and depending on the boundary conditions

$$\begin{aligned}
 u = \lambda u_w(x) = \lambda ax \quad v = -v_w \quad T = T_w \quad \text{at} \quad y = 0 \\
 u \rightarrow 0, \quad T \rightarrow T_\infty \quad \text{as} \quad y \rightarrow \infty.
 \end{aligned}
 \tag{4}$$

with the velocity components in the  $x$  and  $y$  axes denoted as  $u$  and  $v$ , respectively. In the above equations,  $a$  is the constant,  $T$  denotes the temperature of the fluid where  $T_\infty$  denotes the ambient fluid temperature and  $T_w$  is the wall temperature. The shrinking/stretching parameter is denoted as  $\lambda$ . In addition, some parameters that represent the properties of hybrid nanofluid are density  $\rho_{hnf}$ , effective heat capacity  $(\rho C_p)_{hnf}$ , viscosity  $\mu_{hnf}$  and thermal diffusivity  $\alpha_{hnf}$ . The formulation of these parameters is listed in Table 1 while the thermophysical properties of titanium dioxide, copper and the base fluid (water) are provided in Table 2.

**Table 1**  
 Formulations for nanofluid and hybrid nanofluid [23]

Properties	Nanofluid	Hybrid nanofluid
Density	$\rho_{nf} = (1 - \phi_1) \rho_f + \phi_1 \rho_{s1}$	$\rho_{hnf} = (1 - \phi_2) [(1 - \phi_1) \rho_f + \phi_1 \rho_{s1}] + \phi_2 \rho_{s2}$
Heat capacity	$(\rho C_p)_{nf} = (1 - \phi_1) (\rho C_p)_f + \phi_1 (\rho C_p)_{s1}$	$(\rho C_p)_{hnf} = (1 - \phi_2) \left[ (1 - \phi_1) (\rho C_p)_f + \phi_1 (\rho C_p)_{s1} \right] + \phi_2 (\rho C_p)_{s2}$
Viscosity	$\mu_{nf} = \frac{\mu_f}{(1 - \phi_1)^{2.5}}$	$\mu_{hnf} = \frac{\mu_f}{(1 - \phi_1)^{2.5} (1 - \phi_2)^{2.5}}$
Thermal Conductivity	$k_{nf} = \frac{k_{s1} + 2k_f - 2\phi_1(k_f - k_{s1})}{k_{s1} + 2k_f + \phi_1(k_f - k_{s1})} \times k_f$	$k_{hnf} = \frac{k_{s2} + 2k_{nf} - 2\phi_2(k_{nf} - k_{s2})}{k_{s2} + 2k_{nf} + \phi_2(k_{nf} - k_{s2})} \times k_{nf}$ where $k_{nf} = \frac{k_{s1} + 2k_f - 2\phi_1(k_f - k_{s1})}{k_{s1} + 2k_f + \phi_1(k_f - k_{s1})} \times k_f$

**Table 2**  
 Thermophysical properties of the nanoparticles and fluid [24]

Properties	$\rho (kgm^{-3})$	$C_p (Jkg^{-1}K^{-1})$	$k (Wm^{-1}K^{-1})$
TiO <sub>2</sub> (Titanium Dioxide - s1)	4250	8.9538	686.2
Cu (Copper - s2)	8933	385	400
Water (f)	997.1	4179	0.613

The stream function and similarity transformations are introduced to solve Eq. (1) to Eq. (3) through Eq. (4):

$$u = axf'(\eta), \quad v = -\sqrt{av_f} \cdot f(\eta), \quad \eta = y \sqrt{\frac{a}{v_f}}, \quad \theta(\eta) = \frac{T - T_\infty}{T_w - T_\infty}
 \tag{5}$$

where primes denotes differentiation with respect to  $\eta$ . It means that, we can consider the mass flux velocity as

$$v_w = \sqrt{av_f} S.
 \tag{6}$$

Then, the Eq. (2) and Eq. (3) are reduced to the following ordinary differential equations

$$\frac{\mu_{hmf} / \mu_f}{\rho_{hmf} / \rho_f} f''' + ff'' - f'^2 = 0, \quad (7)$$

$$\frac{k_{hmf} / k_f}{Pr(\rho C_p)_{hmf} / (\rho C_p)_f} \theta'' + f\theta' + \frac{Ec}{(1-\phi_1)^{2.5}(1-\phi_2)^{2.5}(\rho C_p)_{hmf} / (\rho C_p)_f} f''^2 = 0 \quad (8)$$

and the boundary conditions become

$$\begin{aligned} f(0) = S, \quad f'(0) = \lambda, \quad \theta(0) = 1, \\ f'(\eta) \rightarrow 0, \quad \theta(\eta) \rightarrow 0 \quad \text{as } \eta \rightarrow \infty. \end{aligned} \quad (9)$$

where  $Pr = \frac{\nu_f}{\alpha_f}$  is Prandtl number,  $S = \frac{v_w}{\sqrt{av_f}}$  is suction parameter and  $Ec = \frac{u_w^2}{(C_p)_f(T_w - T_\infty)}$  is Eckert number. The physical quantities of interest are skin friction coefficient and Nusselt number which are given by

$$C_f = \frac{\mu_{hmf} \left( \frac{\partial u}{\partial y} \right)_{y=0}}{\rho_f \cdot u_w^2}, \quad Nu_x = - \frac{xk_{hmf} \left( \frac{\partial T}{\partial y} \right)_{y=0}}{k_f(T_w - T_\infty)}.$$

Hence

$$Cf_x \sqrt{Re_x} = \frac{f''(0)}{(1-\phi_1)^{2.5}(1-\phi_2)^{2.5}}, \quad \frac{Nu_x}{\sqrt{Re_x}} = - \frac{k_{hmf}}{k_f} \theta'(0) \quad (10)$$

where  $Re_x = xu_w / \nu_f$  is the local Reynolds number.

### 3. Stability Analysis

The stability test was studied by Merkin [25] and continuing extends until now. Based on several researches, most all the first/upper solution defined the status as stable while the second/lower solution is always not stable. In order to figure out the features of stability, the unsteady form for Eq. (2) and Eq. (3) are considered as follows:

$$\frac{\partial u}{\partial t} + u \frac{\partial u}{\partial x} + v \frac{\partial u}{\partial y} = \frac{\mu_{hmf}}{\rho_{hmf}} \frac{\partial^2 u}{\partial y^2} \quad (11)$$

$$\frac{\partial T}{\partial t} + u \frac{\partial T}{\partial x} + v \frac{\partial T}{\partial y} = \alpha_{hmf} \frac{\partial^2 T}{\partial y^2} + \frac{\mu_{hmf}}{(\rho C_p)_{hmf}} \left( \frac{\partial u}{\partial y} \right)^2, \quad (12)$$

By introducing the new similarity variables

$$\begin{aligned}
 u &= ax \frac{\partial f}{\partial \eta}(\eta, \tau), & v &= -\sqrt{av_f} f(\eta, \tau), \\
 \theta(\eta, \tau) &= \frac{T - T_\infty}{T_w - T_\infty}, & \eta &= \sqrt{\frac{a}{v_f}} y, & \tau &= at
 \end{aligned}
 \tag{13}$$

Substitute the Eq. (13) into Eq. (12) and Eq. (13) respectively, we will get

$$\frac{\mu_{hmf} / \mu_f}{\rho_{hmf} / \rho_f} \frac{\partial^3 f}{\partial \eta^3} + f \frac{\partial^2 f}{\partial \eta^2} - \left( \frac{\partial f}{\partial \eta} \right)^2 - \frac{\partial^2 f}{\partial \eta \partial \tau} = 0
 \tag{14}$$

$$\frac{k_{hmf} / k_f}{Pr(\rho C_p)_{hmf} / (\rho C_p)_f} \frac{\partial^2 \theta}{\partial \eta^2} + f \frac{\partial \theta}{\partial \eta} + \frac{Ec}{(1-\phi_1)^{2.5} (1-\phi_2)^{2.5} (\rho C_p)_{hmf} / (\rho C_p)_f} \left( \frac{\partial^2 f}{\partial \eta^2} \right)^2 - \frac{\partial \theta}{\partial \tau} = 0,
 \tag{15}$$

and subject to the new boundary conditions

$$\begin{aligned}
 f(0, \tau) &= S, & \frac{\partial f}{\partial \eta}(0, \tau) &= \lambda & \theta(0, \tau) &= 1, \\
 \frac{\partial f}{\partial \eta}(\eta, \tau) &\rightarrow 0, & \theta(\eta, \tau) &\rightarrow 0 & \text{as } \eta &\rightarrow \infty
 \end{aligned}
 \tag{16}$$

In order to obtain the steady flow solution's stability and satisfying Eq. (7) and Eq. (8), the following functions have been introduced

$$\begin{aligned}
 f(\eta, \tau) &= f_0(\eta) + e^{-\gamma\tau} F(\eta), \\
 \theta(\eta, \tau) &= \theta_0(\eta) + e^{-\gamma\tau} G(\eta),
 \end{aligned}
 \tag{17}$$

where  $F(\eta)$  and  $G(\eta)$  are small relative with  $f_0(\eta)$  and  $\theta_0(\eta)$  respectively. The  $\gamma$  is an unknown eigenvalue parameter and it is notice that there are an infinite set of eigenvalues  $\gamma_1 < \gamma_2 < \gamma_3 \dots$ . Since  $\tau \rightarrow \infty, e^{-\gamma\tau} \rightarrow 0$ , then, by substituting Eq. (17) into Eq. (14) and Eq. (15) that correspond to the boundary conditions (16), we will have the following linear eigenvalue problems

$$\frac{\mu_{hmf} / \mu_f}{\rho_{hmf} / \rho_f} F''' + f_0 F'' + F f_0'' - 2f_0' F' + \gamma F' = 0,
 \tag{18}$$

$$\frac{k_{hmf} / k_f}{Pr(\rho C_p)_{hmf} / (\rho C_p)_f} G'' + f_0 G' + F \theta_0' + \frac{Ec}{(1-\phi_1)^{2.5} (1-\phi_2)^{2.5} (\rho C_p)_{hmf} / (\rho C_p)_f} (2f_0'' F'') + \gamma G = 0
 \tag{19}$$

along with the following boundary conditions

$$\begin{aligned}
 F(0) &= 0, & F'(0) &= 0, & G(0) &= 0, \\
 F'(\infty) &\rightarrow 0, & G(\infty) &\rightarrow 0
 \end{aligned}
 \tag{20}$$

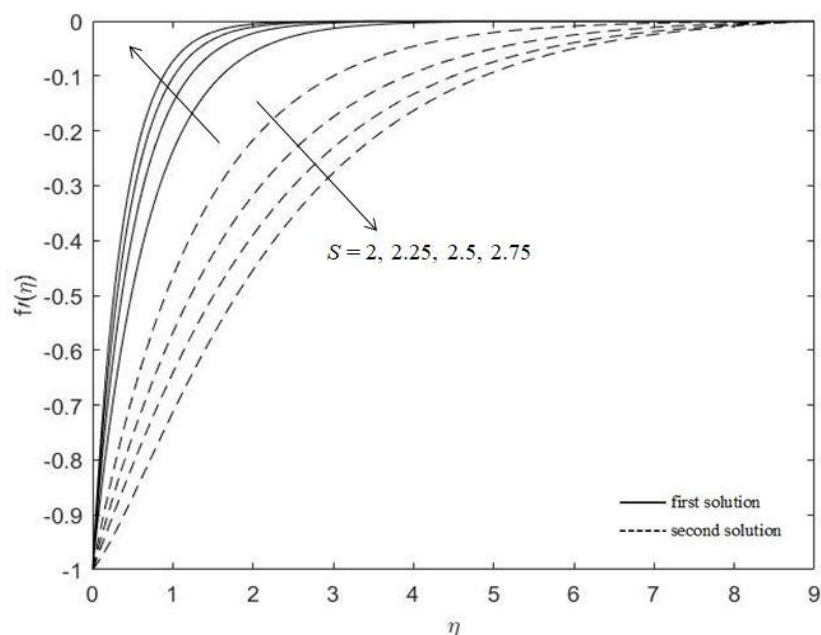
Finally, the condition  $F'(\infty) \rightarrow 0$  is replaced by the stabilizing boundary condition  $F''(0)=1$ . The stability of the dual solutions can be distinguished through the sign of eigenvalue and if the smallest eigenvalue is positive then the solution can be declared as stable solution; otherwise, the negative smallest eigenvalue will be classified as unstable solution.

#### 4. Results and Discussion

The ordinary differential equations (7) and (8) in consort with the boundary conditions (9) are solved numerically using the MATLAB software with the execution of bvp4c programming codes. The suitable initial guesses for  $f''(0)$  and  $-\theta'(0)$  are established to satisfy the asymptotic boundary conditions. The tolerance limit of  $10^{-5}$  is applied throughout the programming process to generate the numerical first and second solutions as well as the velocity and temperature profiles.

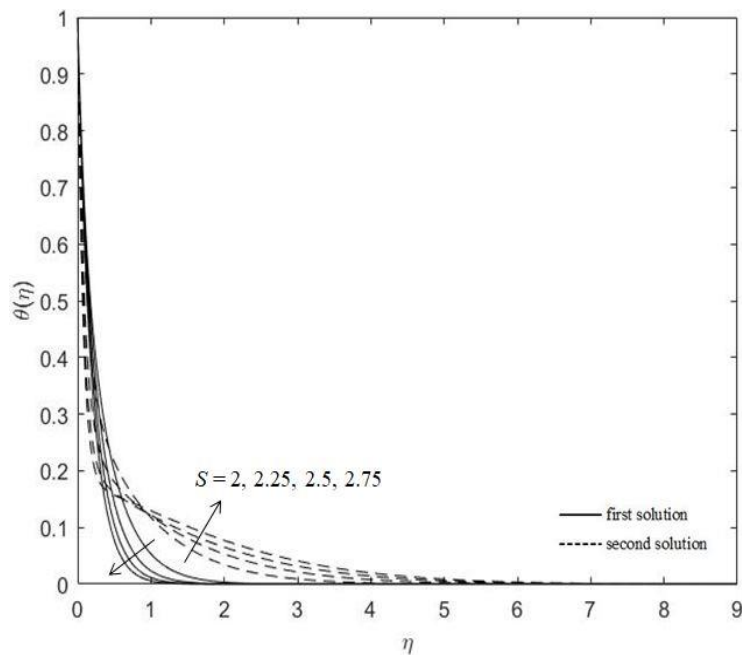
The graphical analysis of the boundary layer flow of copper-titanium oxide (Cu-TiO<sub>2</sub>) hybrid nanofluid with the impact of viscous dissipation are also conducted. Since the base fluid is water (H<sub>2</sub>O), thus Prandtl number used in this study is 6.2. In addition, the effect of the other parameters like suction and nanoparticle volume fraction to the reduced skin friction coefficient  $f''(0)$ , reduced Nusselt number  $-\theta'(0)$ , velocity distribution profile  $f'(\eta)$  and temperature distribution profile  $\theta(\eta)$  also been explored.

Figure 2 and Figure 3 present the velocity and temperature profiles of suction parameter, respectively. In Figure 2, it is clearly seen that the first solution and second solution having the opposite behavior as the first solution shows the velocity increases as suction parameter increases. Conversely, a decrement result obtained for the second solution.



**Fig. 2.** The trend of velocity profile  $f'(\eta)$  with variation in suction parameter

At the same time, in Figure 3, the greater the suction parameter imposes, the first solution is reducing the thickness of thermal boundary layer but contradict results are observed for the second solution where the thermal boundary layer becomes thickened as increasing of suction parameter.



**Fig. 3.** The trend of temperature profile  $\theta(\eta)$  with variation in suction parameter

The dual solutions of velocity and temperature profiles for variation in the copper nanoparticle volume fraction are shown in Figure 4 and Figure 5, respectively. The trend of the velocity profile shown in Figure 4 is similar to Figure 2. In Figure 5, the thermal boundary layer increases as the copper nanoparticles volume fraction increases.

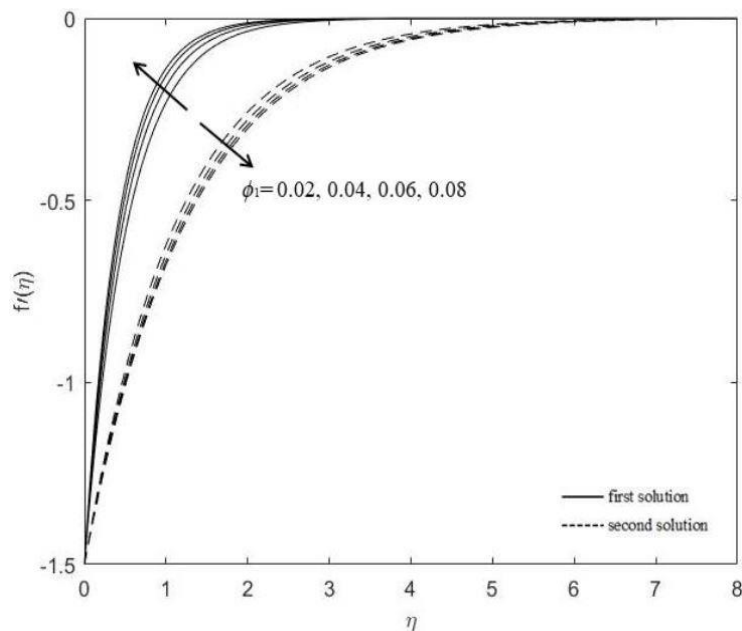


**Fig. 4.** The trend of velocity profile  $f'(\eta)$  with variation in copper nanoparticle volume fraction



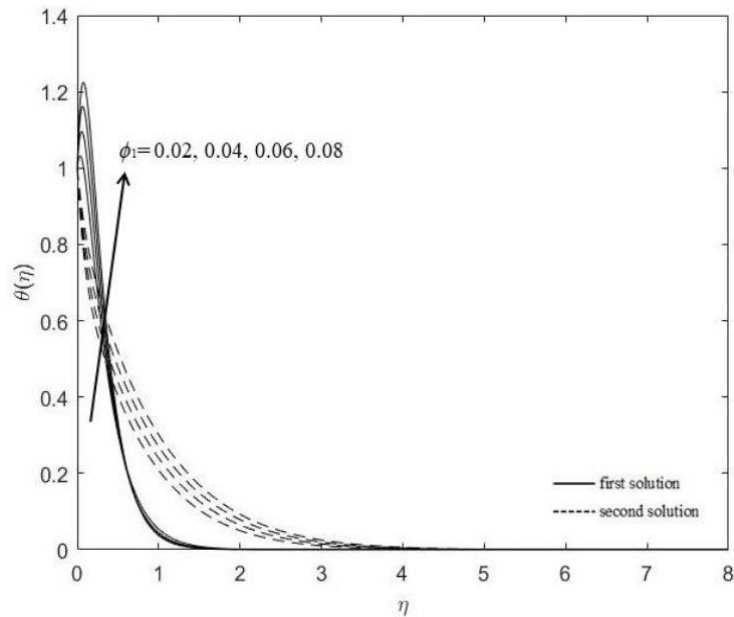


**Fig. 5.** The trend of temperature profile  $\theta(\eta)$  with variation in copper nanoparticle volume fraction

Figure 6 and Figure 7 depict the velocity and temperature profiles of titanium oxide nanoparticle volume fraction, respectively. It is found that the dual solutions show the similar behavior for both profiles. As titanium oxide volume fraction increases, the thickness of momentum boundary layer decreases, however, there is a prominent increment in the thickness of thermal boundary layer.

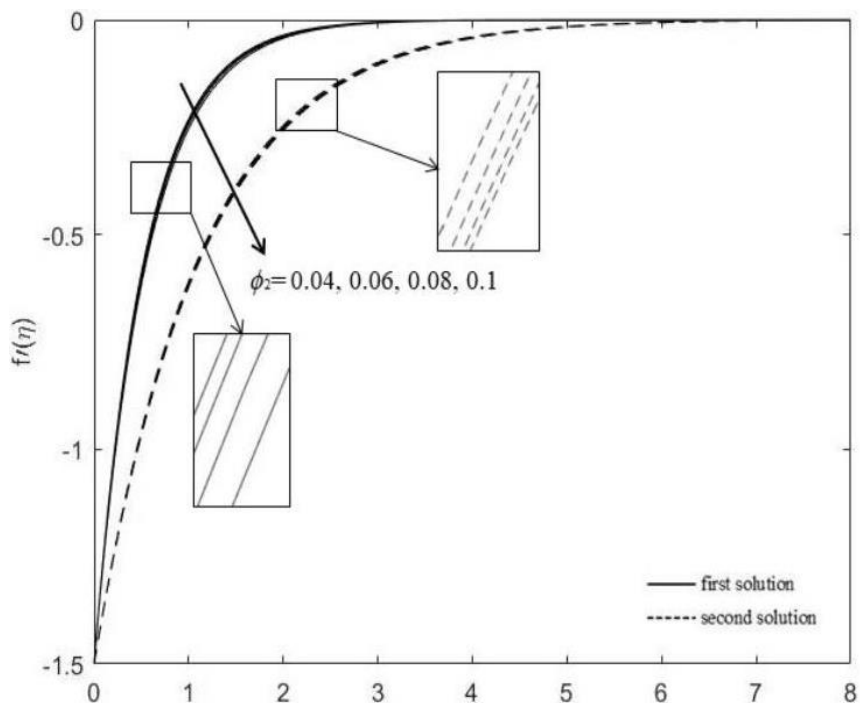


**Fig. 6.** The trend of velocity profile  $f'(\eta)$  with variation in titanium oxide nanoparticle volume fraction

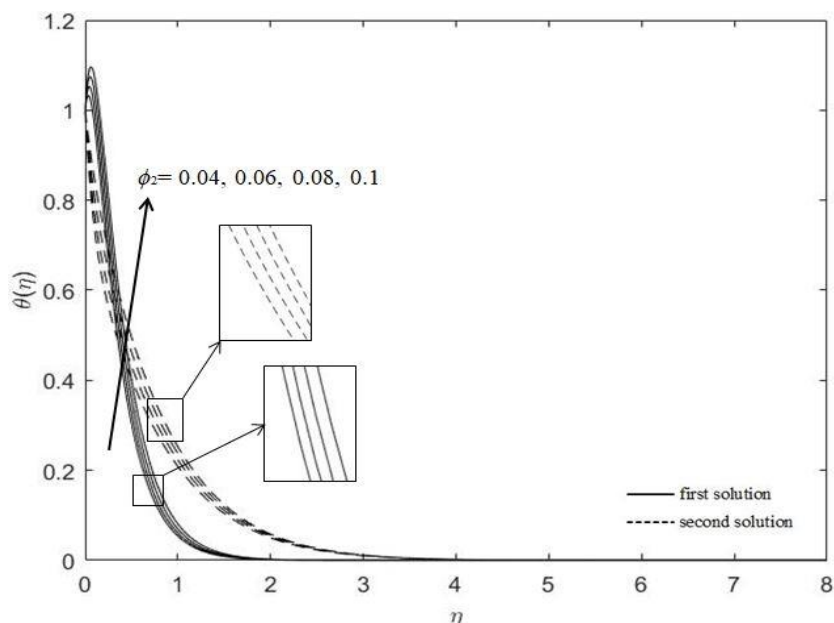


**Fig. 7.** The trend of temperature profile  $\theta(\eta)$  with variation in titanium oxide nanoparticle volume fraction

Besides, the temperature profile of Eckert number has been portrayed in Figure 8. The fluid’s flow temperature profile increases for both solutions as Eckert number escalates all the time.

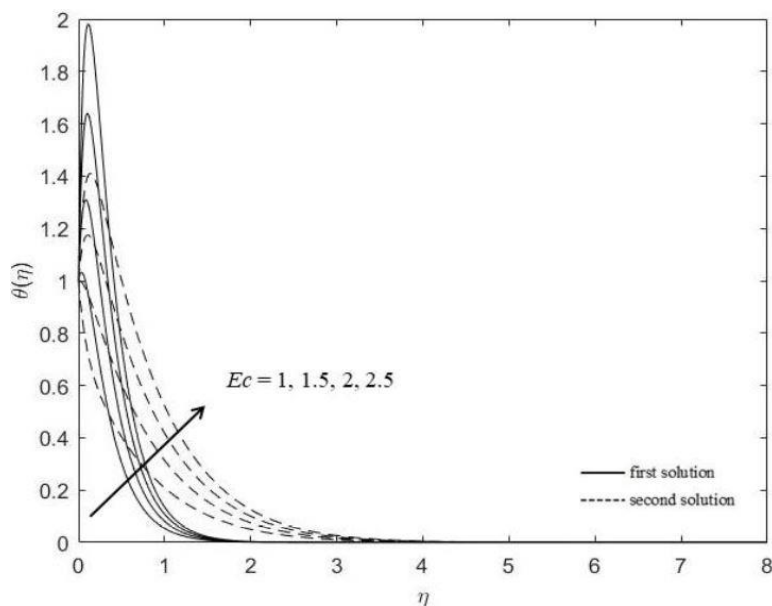


**Fig. 8.** The trend of temperature profile  $\theta(\eta)$  with variation in Eckert number

Figure 9 and Figure 10 depict dual solutions for various value of suction parameter  $s$  with the shrinking/stretching parameter  $\lambda$  on  $f''(0)$  and  $-\theta'(0)$ , respectively. From the both graphs, it can be seen that there is a unique solution exists for the first and second solution up on  $\lambda_c$ , the critical value. Meanwhile, the solutions only discovered when  $\lambda \geq \lambda_c$ . Based on the graph, it can be noticed that the higher value of suction parameter  $S = 2.75$  contributes to the smaller critical value  $\lambda_c = -2.0829$ . Furthermore, based on the Figure 9, it obviously portrayed that when the sheet is stretched ( $\lambda > 0$ )

and shrunk ( $\lambda < 0$ ), the magnitude of the reduced skin friction coefficient  $|f''(0)|$  increases as the suction parameter increases but the trend has the opposite behavior for reduced Nusselt number which shown in Figure 10.

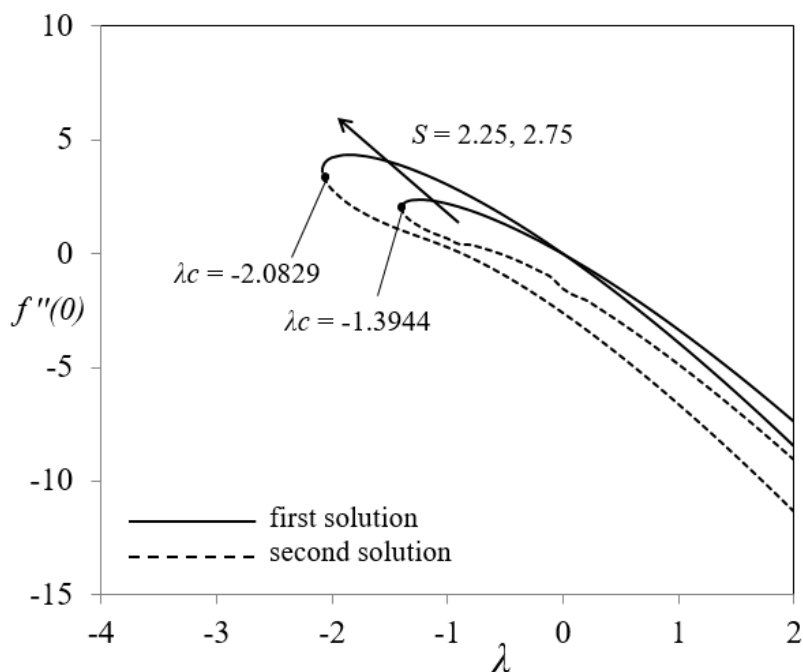


Fig. 9. Variations of  $f''(0)$  for several values of suction parameter

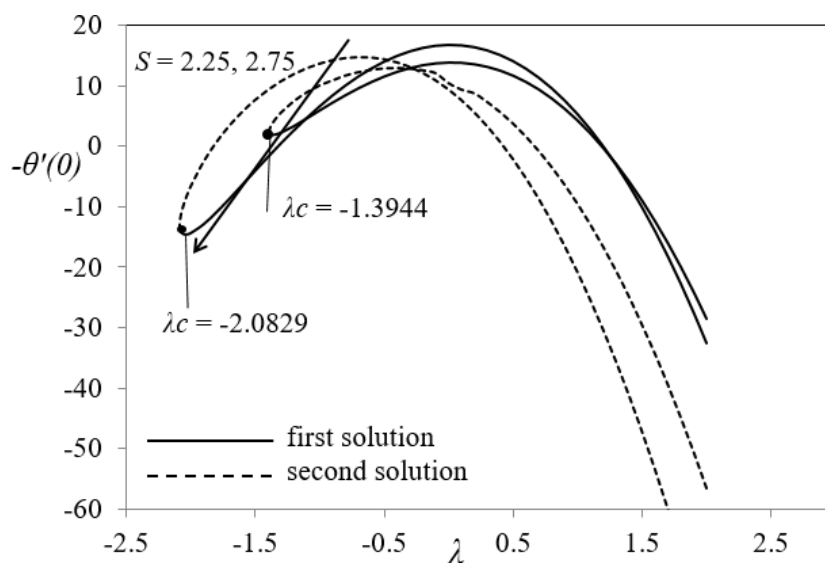
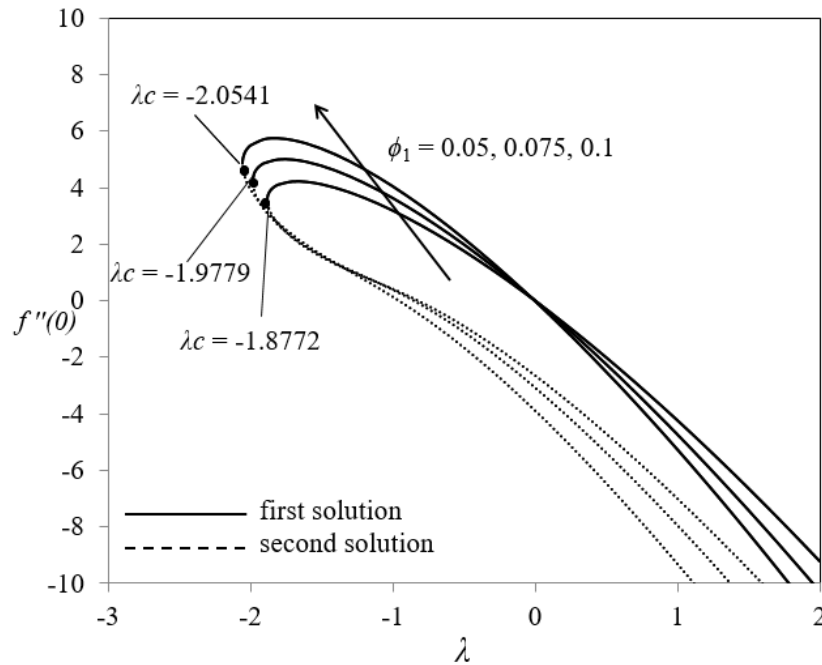


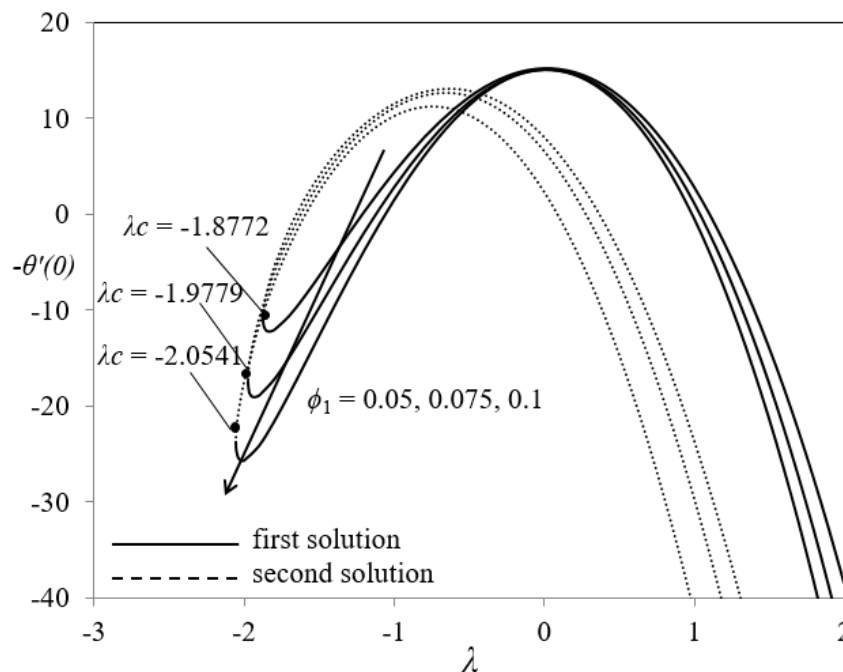
Fig. 10. Variations of  $-\theta'(0)$  for several values of suction parameter

Figure 11 and Figure 12 illustrate the influence of copper (Cu) nanoparticle volume fraction on suction parameter with reduced skin friction coefficient and Nusselt number, respectively. The magnitude of the reduced skin friction coefficient  $|f''(0)|$  increases as the copper nanoparticles concentration increases as depicted in Figure 11. The critical values are -1.8772, -1.9779 and -2.0541 which correspond to  $\phi_1$  equals to 0.05, 0.1 and 0.15, respectively. For Figure 12, the reduced Nusselt number decreases at the both of stretching or shrinking sheet when the copper nanoparticles concentration increases. This result refutes the statement that increasing the concentration of

nanoparticles able to enhance the heat transfer. The same results had been obtained by the previous researchers and they deduced that this phenomenon might be caused by the chosen values of governing parameter [26]. Thus, this result somewhat show that the hybrid nanofluid could not enhance the heat transfer rate optimally if not under the satisfied conditions.



**Fig. 11.** Variations of  $f''(0)$  for several values of copper nanoparticle volume fraction



**Fig. 12.** Variations of  $-\theta'(0)$  for several values of copper nanoparticle volume fraction

Figure 13 and Figure 14 show the influence of titanium dioxide (TiO<sub>2</sub>) nanoparticle volume fraction on suction parameter with reduced skin friction coefficient and Nusselt number respectively. The critical values are -1.7122, -1.6881 and -1.6528 which correspond to  $\phi_2$  equals to 0.06, 0.09 and 0.12, respectively. The magnitude of the reduced skin friction coefficient  $|f''(0)|$  decreases as the titanium oxide nanoparticles concentration increases as shown in Figure 13. For Figure 14, the reduced Nusselt number decreases as the titanium oxide nanoparticles concentration increases.

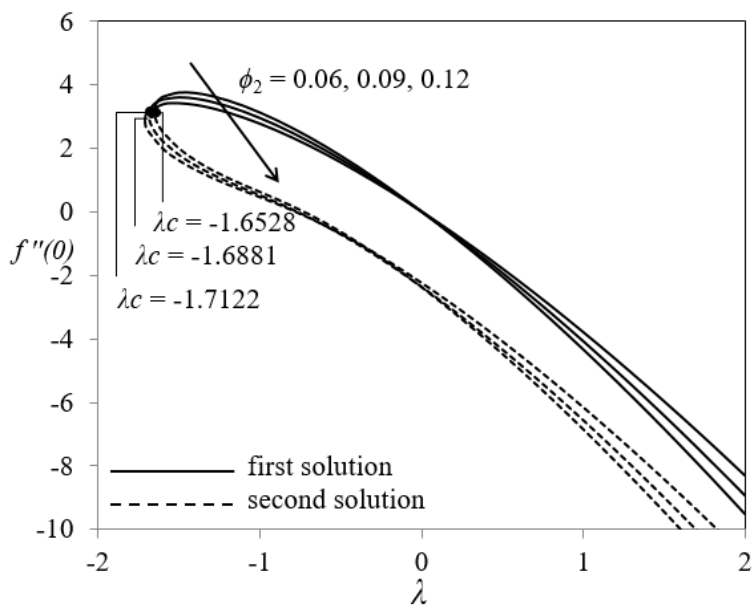


**Fig. 13.** Variations of  $f''(0)$  for several values of titanium oxide nanoparticle volume fraction

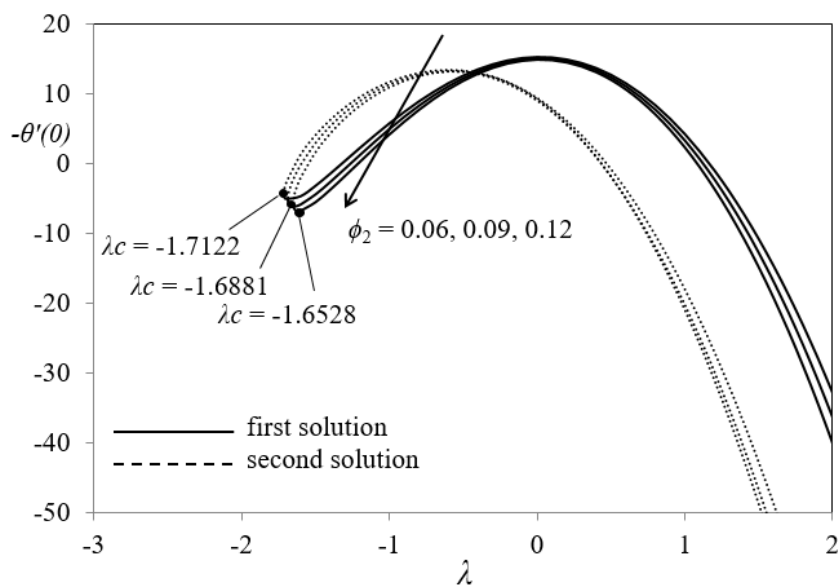


**Fig. 14.** Variations of  $-\theta'(0)$  for several values of titanium oxide nanoparticle volume fraction

As shown in Figure 15, the various values of Eckert number have same exact critical value  $\lambda_c = -1.7214$  for shrinking/stretching parameter  $\lambda$  on the reduced Nusselt number. The presence of viscous dissipation causes the transformation of kinetic energy to heat and contributes the higher temperature to the fluid. At the same time, the Eckert number could be defined as the ratio of kinetic energy and enthalpy which lead to the decrement in heat transfer rate. Therefore, increases in Eckert number causes a decrease in the reduced Nusselt number.

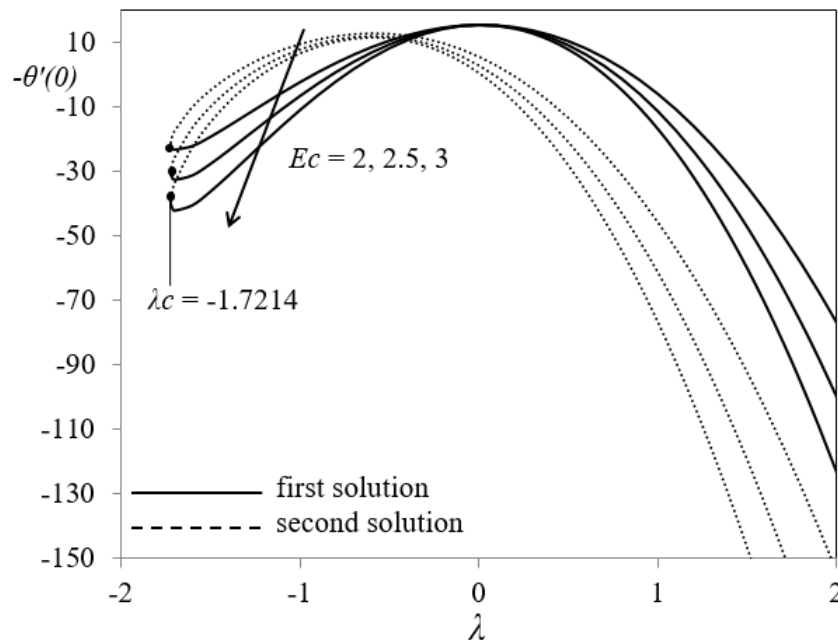


Fig. 15. Variations of  $-\theta'(0)$  for several values of Eckert number

Table 3 shows the computation result of stability analysis for the dual solutions and it is clearly seen that the first solution gives the positive eigenvalue while the second solution produces the negative eigenvalue. As a conclusion, the first solution is stable whereas the second solution is unstable.

**Table 3**

Results of stability analysis when  $Ec = 1, Pr = 6.2, \phi_1 = 0.02, \phi_2 = 0.04$  and  $S = 2.25$

$\lambda$	$\gamma_1$ (1 <sup>st</sup> Solution)	$\gamma_2$ (2 <sup>nd</sup> Solution)
-0.1	3.5611	-0.6478
-0.3	3.4089	-0.6266
-0.5	3.2466	-0.6119
-0.7	2.1847	-0.6058
-0.9	1.3339	-0.5991
-1.1	1.1443	-0.5518
-1.3	0.9038	-0.3725
-1.39	0.0946	-0.0868
-1.394	0.0330	-0.0239
-1.3944	0.0107	-0.000009

## 5. Conclusions

The problem of the boundary layer flow of Cu-TiO<sub>2</sub> hybrid nanofluid with the presence of viscous dissipation had been solved numerically. The prominent of finding results are highlighted as follows

- i. The velocity and temperature profiles for suction parameter showed the opposite trend in dual solutions.
- ii. Cu and TiO<sub>2</sub> nanoparticle volume fraction enlarged the thickness of boundary layer in temperature profile for both solutions.
- iii. The presence of higher concentration Cu and TiO<sub>2</sub> nanoparticles led to a rise in the reduced skin friction coefficient. Also, both nanoparticles contributed to a decrement in the reduced Nusselt number.
- iv. The Eckert number enlarged the thickness of boundary layer in temperature profile for both solutions.
- v. The first solution is more stable than the second solution.

## Acknowledgement

The authors are gratefully acknowledging the financial support from Universiti Malaysia Pahang via the research grant RDU1903143 and RDU213201 in completing this study.

## References

- [1] Mahian, Omid, Lioua Kolsi, Mohammad Amani, Patrice Estellé, Goodarz Ahmadi, Clement Kleinstreuer, Jeffrey S. Marshall et al. "Recent advances in modeling and simulation of nanofluid flows-Part I: Fundamentals and theory." *Physics Reports* 790 (2019): 1-48. <https://doi.org/10.1016/j.physrep.2018.11.004>
- [2] Choi, S. US, and Jeffrey A. Eastman. *Enhancing thermal conductivity of fluids with nanoparticles*. No. ANL/MSD/CP-84938; CONF-951135-29. Argonne National Lab., IL (United States), 1995.
- [3] Ambreen, Tehmina, and Man-Hoe Kim. "Influence of particle size on the effective thermal conductivity of nanofluids: A critical review." *Applied Energy* 264 (2020): 114684. <https://doi.org/10.1016/j.apenergy.2020.114684>
- [4] Hwang, Yu-jin, J. K. Lee, C. H. Lee, Y. M. Jung, S. I. Cheong, C. G. Lee, B. C. Ku, and S. P. Jang. "Stability and thermal conductivity characteristics of nanofluids." *Thermochimica Acta* 455, no. 1-2 (2007): 70-74. <https://doi.org/10.1016/j.tca.2006.11.036>
- [5] Ganvir, R. B., P. V. Walke, and V. M. Kriplani. "Heat transfer characteristics in nanofluid-a review." *Renewable and Sustainable Energy Reviews* 75 (2017): 451-460. <https://doi.org/10.1016/j.rser.2016.11.010>
- [6] Chakraborty, Samarshi, and Pradipta Kumar Panigrahi. "Stability of nanofluid: A review." *Applied Thermal Engineering* 174 (2020): 115259. <https://doi.org/10.1016/j.applthermaleng.2020.115259>
- [7] Hemmati-Sarapardeh, Abdolhossein, Amir Varamesh, Maen M. Husein, and Kunal Karan. "On the evaluation of the viscosity of nanofluid systems: Modeling and data assessment." *Renewable and Sustainable Energy Reviews* 81 (2018): 313-329. <https://doi.org/10.1016/j.rser.2017.07.049>
- [8] Bakthavatchalam, Balaji, Khairul Habib, R. Saidur, Bidyut Baran Saha, and Kashif Irshad. "Comprehensive study on nanofluid and ionanofluid for heat transfer enhancement: A review on current and future perspective." *Journal of Molecular Liquids* 305 (2020): 112787. <https://doi.org/10.1016/j.molliq.2020.112787>
- [9] Zhang, Yun, and Xiaojie Xu. "Predicting the thermal conductivity enhancement of nanofluids using computational intelligence." *Physics Letters A* 384, no. 20 (2020): 126500. <https://doi.org/10.1016/j.physleta.2020.126500>
- [10] Kumar, D. Dhinesh, and A. Valan Arasu. "A comprehensive review of preparation, characterization, properties and stability of hybrid nanofluids." *Renewable and Sustainable Energy Reviews* 81 (2018): 1669-1689. <https://doi.org/10.1016/j.rser.2017.05.257>
- [11] Sajid, Muhammad Usman, and Hafiz Muhammad Ali. "Thermal conductivity of hybrid nanofluids: a critical review." *International Journal of Heat and Mass Transfer* 126 (2018): 211-234. <https://doi.org/10.1016/j.ijheatmasstransfer.2018.05.021>
- [12] Zufar, Muhammad, Prem Gunnasegaran, Khai Ching Ng, and Hemantkumar B. Mehta. "Evaluation of the thermal performance of hybrid nanofluids in pulsating heat pipe." *CFD Letters* 11, no. 11 (2019): 13-24.
- [13] Ali, I. R., Ammar I. Alsabery, N. A. Bakar, and Rozaini Roslan. "Mixed Convection in a Lid-Driven Horizontal Rectangular Cavity Filled with Hybrid Nanofluid By Finite Volume Method." *Journal of Advanced Research in Micro and Nano Engineering* 1, no. 1 (2020): 38-49.

- [14] Khashi'ie, Najiyah Safwa, Ezad Hafidz Hafidzuddin, Norihan Md Arifin, and Nadiyah Wahi. "Stagnation point flow of hybrid nanofluid over a permeable vertical stretching/shrinking cylinder with thermal stratification effect." *CFD Letters* 12, no. 2 (2020): 80-94.
- [15] Huminic, Gabriela, and Angel Huminic. "Hybrid nanofluids for heat transfer applications-a state-of-the-art review." *International Journal of Heat and Mass Transfer* 125 (2018): 82-103. <https://doi.org/10.1016/j.ijheatmasstransfer.2018.04.059>
- [16] Shah, Tayyab Raza, and Hafiz Muhammad Ali. "Applications of hybrid nanofluids in solar energy, practical limitations and challenges: a critical review." *Solar Energy* 183 (2019): 173-203. <https://doi.org/10.1016/j.solener.2019.03.012>
- [17] Farooq, Umer, Muhammad Idrees Afridi, Muhammad Qasim, and D. C. Lu. "Transpiration and viscous dissipation effects on entropy generation in hybrid nanofluid flow over a nonlinear radially stretching disk." *Entropy* 20, no. 9 (2018): 668. <https://doi.org/10.3390/e20090668>
- [18] Jusoh, R., K. Naganthran, A. Jamaludin, M. H. Ariff, M. F. M. Basir, and I. Pop. "Mathematical analysis of the flow and heat transfer of Ag-Cu hybrid nanofluid over a stretching/shrinking surface with convective boundary condition and viscous dissipation." *Data Analytics and Applied Mathematics (DAAM)* 1, no. 01 (2020): 11-22. <https://doi.org/10.15282/daam.v1i01.5105>
- [19] Jahan, Sultana, M. Ferdows, M. D. Shamshuddin, and Khairy Zaimi. "Effects of Solar Radiation and Viscous Dissipation on Mixed Convective Non-Isothermal Hybrid Nanofluid over Moving Thin Needle." *Journal of Advanced Research in Micro and Nano Engineering* 3, no. 1 (2021): 1-11.
- [20] Zokri, Syazwani Mohd, Nur Syamilah Arifin, Abdul Rahman Mohd Kasim, and Mohd Zuki Salleh. "Flow of Jeffrey Fluid over a Horizontal Circular Cylinder with Suspended Nanoparticles and Viscous Dissipation Effect: Buongiorno Model." *CFD Letters* 12, no. 11 (2020): 1-13. <https://doi.org/10.37934/cfdl.12.11.113>
- [21] Venkateswarlu, Bhumavarapu, and Panyam Venkata Satya Narayana. "Cu-Al<sub>2</sub>O<sub>3</sub>/H<sub>2</sub>O hybrid nanofluid flow past a porous stretching sheet due to temperature-dependent viscosity and viscous dissipation." *Heat Transfer* 50, no. 1 (2021): 432-449. <https://doi.org/10.1002/htj.21884>
- [22] Aziz, Asim, Wasim Jamshed, Taha Aziz, Haitham M. S. Bahaidarah, and Khalil Ur Rehman. "Entropy analysis of Powell-Eyring hybrid nanofluid including effect of linear thermal radiation and viscous dissipation." *Journal of Thermal Analysis and Calorimetry* 143, no. 2 (2021): 1331-1343. <https://doi.org/10.1007/s10973-020-10210-2>
- [23] Waini, I., A. Ishak, and I. Pop. "Hybrid nanofluid flow and heat transfer past a permeable stretching/shrinking surface with a convective boundary condition." In *Journal of Physics: Conference Series*, vol. 1366, no. 1, p. 012022. IOP Publishing, 2019. <https://doi.org/10.1088/1742-6596/1366/1/012022>
- [24] Aaiza, Gul, Ilyas Khan, and Sharidan Shafie. "Energy transfer in mixed convection MHD flow of nanofluid containing different shapes of nanoparticles in a channel filled with saturated porous medium." *Nanoscale Research Letters* 10, no. 1 (2015): 1-14. <https://doi.org/10.1186/s11671-015-1144-4>
- [25] Merkin, J. H. "Mixed convection boundary layer flow on a vertical surface in a saturated porous medium." *Journal of Engineering Mathematics* 14, no. 4 (1980): 301-313. <https://doi.org/10.1007/BF00052913>
- [26] Jusoh, Rahimah, Roslinda Nazar, and Ioan Pop. "Magnetohydrodynamic boundary layer flow and heat transfer of nanofluids past a bidirectional exponential permeable stretching/shrinking sheet with viscous dissipation effect." *Journal of Heat Transfer* 141, no. 1 (2019). <https://doi.org/10.1115/1.4041800>